

# Analysis of Wireless Power Transfer Technique in Electric Vehicles for Different Coils without & with Ferromagnetic Core

**Somasree Deb**

Dept. of EE  
Meghnad Saha Institute of Technology  
Kolkata, India

**Ansu Biswas**

Dept. of EE  
Meghnad Saha Institute of Technology  
Kolkata, India

**Mousumi JanaBala**

Dept. of EE  
Meghnad Saha Institute of Technology  
Kolkata, India

**Epsita Das**

Dept. of EE  
Meghnad Saha Institute of Technology  
Kolkata, India

**Sayanti Maulik**

Dept. of EE  
Meghnad Saha Institute of Technology  
Kolkata, India

**Kaustuv Dasgupta**

Dept. of EE  
Meghnad Saha Institute of Technology  
Kolkata, India

**Abstract**—Electric Vehicle (EV) charging stations are gaining popularity to meet the needs of the hour for EVs. In India, the number of EV charging stations almost doubled from 6586 to 12,146 in the span of the last one year, as per the statistics given by the Ministry of Power, India. The Ministry of Heavy Industries approved a large subsidy of Rs. 800 crores to install 7,432 EV charging stations. Wireless EV charging is advancing very fast because of its advantages of reducing wear and tear and increasing convenience and facility to charge the vehicle while in motion. This paper analysed the Inductive Wireless Power Transfer (IWPT) method for different coil structures. The operating principle of IWPT is similar to that of the transformer; only the ferrite core is absent here. The absence of ferromagnetic material leads to a low coupling coefficient. Therefore, a compensation circuit becomes necessary to compensate for the low coupling coefficient. However, a ferrite core in the inductor coil exhibits higher magnetic permeability than the air-cored inductor. The magnitudes of the inductances also depend on the coils' shape. In this research, the circular and rectangular shape of the transmitter and receiver coils have been analysed in the Ansys Maxwell environment. The finite element analysis (FEA) was carried out in Magnetostatics mode. The mutual and self-inductances for the rectangular coil are higher than that of the circular coil, considering the same number of turns and current magnitude in both coils.

**Keywords**— Circular Planar Coil, Electric Vehicle, Ferrite Core, Inductive Wireless Power Transfer, Magnetic Coupling, Rectangular Planar Coil.

## I. INTRODUCTION

Electric vehicles (EVs) are gradually gaining popularity in India. A sufficient number of EV charging stations is crucial to maintain this growth. Two methods for EV charging are wired and wireless. Wired EV charging systems are highly reliable but suffer from cable resistance, voltage regulation, and heat management problems. With advancements in technology, wireless EV charging is growing very fast. Researchers are searching for ways to improve wireless EV charging system efficiency. Research is

progressing in multiple directions to enhance wireless charging efficiency, considering the WPT technology [1]-[2], transmitter and receiver coil design, compensation circuit design [3], etc. Literatures are categorised on the basis of charging methods used and their analysis. EVs' Wireless Power Transfer (WPT) are divided into i) electromagnetic induction and ii) electrostatic induction. Further, the electromagnetic induction method is subdivided into i) inductive coupling and ii) magnetic resonant coupling, as shown in Fig.1. The charging system can only go from grid to EV or vice versa. A bidirectional Inductive Wireless Power Transfer (IWPT) model between grid and EV is proposed in [4]. This paper demonstrates a novel IWPT method for EV charging. Two inductive coils are used in IWPT. The coil attached to the voltage source is called the transmission coil (TC). The other one, the receiver coil (RC), is electrically isolated from the TC and kept at a distance in the air, as shown in Fig.2. It is called a loosely coupled system. The magnetic linkage coefficient in a loosely coupled system is low. A ferrite core coil is a solution to this problem [5]. Researchers proposed several design ideas for IWPT technique based on coil structure[6], coil distance [7], misalignment[1] etc. High-frequency AC voltage is applied to the loosely coupled air-cored coil to increase magnetic linkage with the receiver. Researchers are working on different optimisation techniques for coil design [8]. A high-frequency inverter increases the magnetic coupling coefficient. A self-oscillating controlled inverter is proposed in [9] for a robust, efficient IWPT system.

However, high frequency leads to more core losses. The researchers also explore lower frequency ranges like 50Hz. Low-frequency metamaterial is used in IWPT; however, its application is more in bio-engineering as low frequency is inevitable to avoid settling high-frequency power in biological tissues [10]. A 50Hz WPT is developed to transfer 300kW power to a railway car as reported by Yoda [11]. The

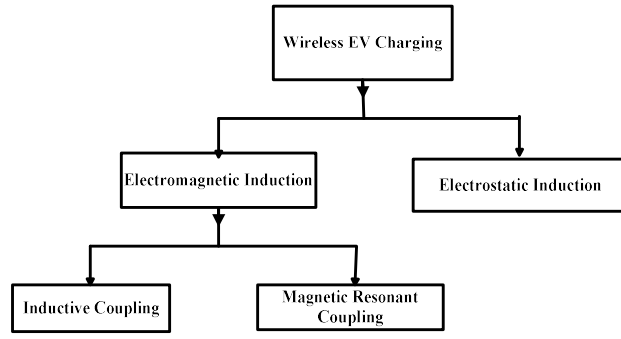


Fig. 1. IWPT methods for EV charging

operating principle of WPT is similar to that of the transformer; only the ferrite core is absent here.

The absence of ferromagnetic material leads to a low coupling coefficient. Therefore, a compensation circuit becomes necessary to compensate for the low coupling coefficient [12]. However, a ferrite core in the inductor coil exhibits higher magnetic permeability than the air-cored inductor. Studies are going to optimise the dimension and design of the coil structure of the WPT system [13].

This paper analysed the comparative study between circular and rectangular planar coils in wireless EV charging application. The study compares the mutual, self-inductances, coupling coefficient for both the coils and effective flux linkage for the RC considering same coil currents and number of turns.

## II. MUTUAL INDUCTANCE WIRELESS POWER TRANSFER

Fig. 2. illustrates the components of the WPT scheme. The system has a transmitter coil (TC) and a receiver coil (RC). An AC supply of 50 Hz is first rectified via a rectifier unit. DC is then fed to an inverter to produce a high-frequency AC. High frequency improves the power transfer efficiency. The compensation circuit eliminates the voltage drop caused in the circuit. Compensating circuit is followed by the TC and RC coils for the IWPT. A change in current magnitude in the TC induces a voltage in the RC. The coupling factor  $k$  is defined as:

$$k = \frac{M}{\sqrt{L_T L_R}} \quad (1)$$

where  $L_T$  is the inductance of TC

$L_R$  is the inductance of RC

$M$  is the mutual inductance between two coils and

$0 \leq k \leq 1$

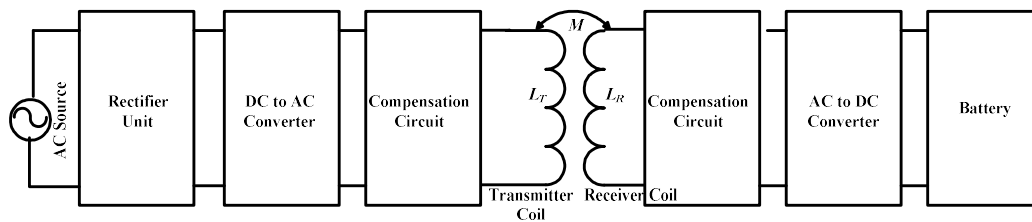


Fig. 2. Schematic diagram for IWPT

Equation (1) indicates that  $k$  depends upon the size of the inductor coils and the distance between them. A DC-to-AC converter and battery compensation network follow the RC coil. In this paper, two differently shaped coil structures are analysed. They are

- i) Circular Planar coil
- ii) Rectangular Planar coil

Fig.3 and 4 shows the different variables associated with the inductance calculations of two different coil structures studied in this work.

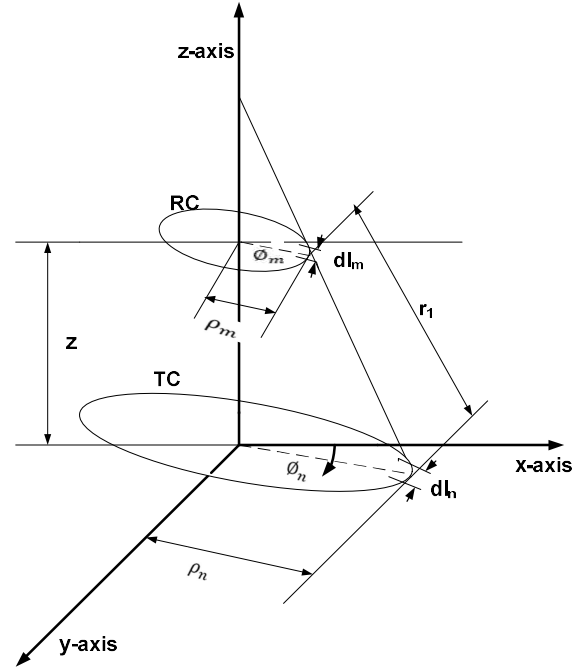


Fig. 3. Mutual inductance for circular planar coil

### A. Self Inductance

The self-inductance of a circular coil is

$$L = \frac{n\Phi}{i} \quad (2)$$

$$L_c = n \frac{\pi \mu_0 \frac{nir}{2}}{i} = \pi \mu_0 \frac{n^2 r}{2} \quad (3)$$

where  $r$  is the radius of the circular coil and  $\mu_0$  is the permeability of air. Similarly, self-inductance of a rectangular loop is:

$$L_r = \mu_0 \frac{a}{\pi} \ln\left(\frac{b}{r}\right) \quad (4)$$

where  $a$  and  $b$  are the length and breath, respectively,  $r$  is radius of the conductor.

### B. Mutual Inductance in Circular Coil

The mutual inductance between two current-carrying loops of RC and TC as shown in Fig.3 was obtained with the help of the following formula [13].

$$M = \frac{\mu_0}{4\pi} \oint_{C_1} \oint_{C_2} \frac{dl_n dl_m}{r_l} \quad (5)$$

where, the  $n^{\text{th}}$  and  $m^{\text{th}}$  loops are considered for TC and RC respectively.

$r_l$  is the distance between the line element  $dl_n$  and  $dl_m$ . In the given design, if we consider one loop of coil 1 (say  $n^{\text{th}}$  loop) and one loop of coil 2 (say  $m^{\text{th}}$  loop), then the mutual inductance between these two loops was formulated from eqn. 5.

$$M_{nm} = \frac{\mu_0 \rho_n \rho_m}{4\pi} \int_{\phi_n=0}^{2\pi} \int_{\phi_m=0}^{2\pi} \frac{d\phi_n d\phi_m}{\sqrt{(x_n - x_m)^2 + (y_n - y_m)^2 + z^2}} \quad (6)$$

where,

$$x_n = \rho_n \cos \phi_n, x_m = \rho_m \cos \phi_m,$$

$$y_n = \rho_n \sin \phi_n, y_m = \rho_m \sin \phi_m$$

Where  $\rho_n$  and  $\rho_m$  are the radii of tow loops respectively and  $z$  is the axial distance. If we consider the radius of the inner core is  $\rho_0$  and the diameter of the copper wire of the coil is  $d$ , then the radii were expressed by the following equations.

$$\rho_n = \rho_0 + nd \quad \text{and} \quad \rho_m = \rho_0 + md \quad (7)$$

Total mutual inductance, hence can be determined.

$$M = \sum_{n=0}^{N_1} \sum_{m=0}^{N_2} M_{nm} \quad (8)$$

$N_1$  and  $N_2$  are the total number of coils of coil 1 and 2, respectively.

### C. Mutual Inductance in Rectangular Coil

Similarly, for the concentric rectangular coils, as shown in Fig. (4) the mutual inductance for loop of coil 1 (say  $n^{\text{th}}$  loop) and one loop of coil 2 (say  $m^{\text{th}}$  coil) was obtained from equ (9).

$$M_{nm} = \frac{\mu_0}{2\pi} \left[ \int_{y_n=-b_n}^{b_n} \int_{y_m=-b_m}^{b_m} \frac{dy_n dy_m}{\sqrt{(a_n-a_m)^2 + (y_n-y_m)^2 + z^2}} + \int_{x_n=-a_n}^{a_n} \int_{x_m=-a_m}^{a_m} \frac{dx_n dx_m}{\sqrt{(b_n-b_m)^2 + (x_n-x_m)^2 + z^2}} + \int_{y_n=-b_n}^{b_n} \int_{y_m=-b_m}^{b_m} \frac{dy_n dy_m}{\sqrt{(a_n+a_m)^2 + (y_n-y_m)^2 + z^2}} + \int_{x_n=-a_n}^{a_n} \int_{x_m=-a_m}^{a_m} \frac{dx_n dx_m}{\sqrt{(b_n+b_m)^2 + (x_n-x_m)^2 + z^2}} \right] \quad (9)$$

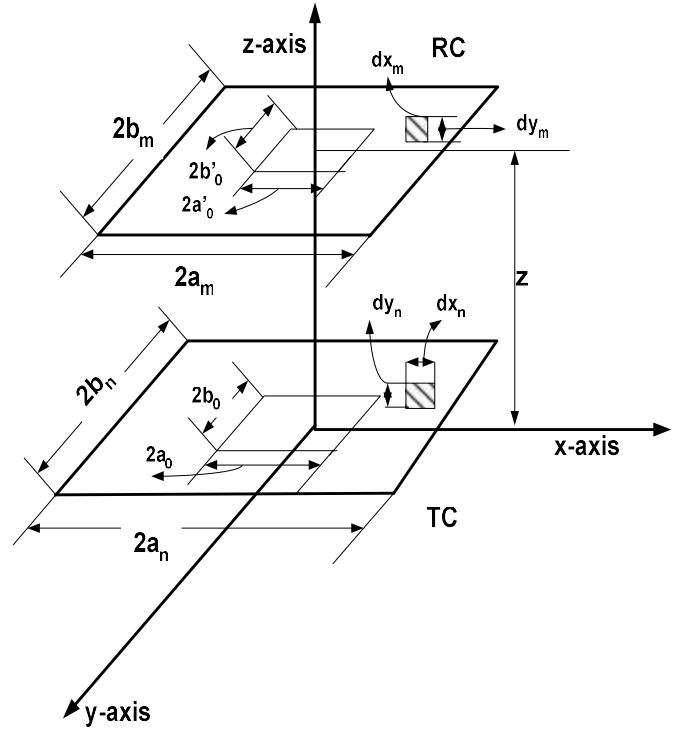


Fig. 4. Mutual inductance for rectangular planar coil

where  $2a_n$  and  $2b_n$  are the length and width of the loop 1 and  $2a_m$  and  $2b_m$  are the length and width of loop 2, respectively. If the inner core length and width of coil 1 are  $2a_0$ ,  $2b_0$  and the inner core length and width of coil 2 are  $2a'_0$ ,  $2b'_0$  respectively, while the diameter of each copper wire is  $d$ , then we can express  $a_n$  and  $b_n$  by eqn. (10) and  $a_m$  and  $b_m$  by eqn. 11.

$$a_n = a_0 + nd \quad \text{and} \quad b_n = b_0 + nd \quad (10)$$

$$a_m = a'_0 + md \quad \text{and} \quad b_m = b'_0 + md \quad (11)$$

Total mutual inductance was computed again using eqn (8).

## III. SIMULATION & ANALYSIS

Two sets of identical planar coils, circular and rectangular, with and without core, were designed and then simulated in the Ansys Maxwell environment. The focus is to obtain the steady-state analysis of the coils. Magnetostatics analysis with current excitation is typically used in the Maxwell environment for this kind of analysis. The number of turns, cross-sectional area of the conductor, diameter of the TC and RC, the intermediate distance between the coils, current through the coils etc., all the specifications are identical for both sets of the coils. The detailed specifications of the transmitter and receiver coil with and without core have been tabulated in Table 1.

First, the coils were excited without a ferromagnetic core. The flux flow is modified by introducing a small piece of ferromagnetic core within the coils, as shown in Fig.5 and 6. Integration of the magnetic core eases the flow of the magnetic flux from the TC to the RC by reducing the

reluctance of the magnetic path. In this analysis, the selection of ferromagnetic core structure is based on the inner diameter of the coil. The flux produced by the transmitting coil will link the receiver coil to induce the emf for charging the battery of the electric vehicles.

Here, the increment of the flux linkages with the RC is intended, which has been obtained by introducing the magnetic core and changing the shape of the coil. Although two coil structures have the same number of turns and the same cross-sectional area of the conductor, the coil surface area is different due to their shape, so the magnetic flux changes. In this case, the surface area of the rectangular coil is greater, and the mutual and self-inductances are more significant, which results in an increment of the mutual and self-inductances. The magnitude of the mutual inductances has been increased by approximately 7.93 times for the air core and approximately 19.03 times for M43\_29G. The magnetostatics analysis in the Maxwell environment is given in Table 2.

**Table 1: Specification of the WPT Planar Coil**

Parameter	Value	Unit
No of turns, Transmitter/Receiver	20/10	
Cross sectional area of the conductor, Transmitter/Receiver	1/0.5	mm <sup>2</sup>
Diameter of the circular coils, Transmitter/Receiver	24/12	mm
Dimensions of the rectangular coils Transmitter/Receiver	36x27/22x21	mm <sup>2</sup>
Intermediate distance between the coils	50	mm
Material of the coil	Copper	
Core Material	M43_29G	
Core dimension for circular coil diameter × height	5.5×5	mm/mm
Core dimension for rectangular coil diameter/height	5.5×5×5	mm/mm/mm

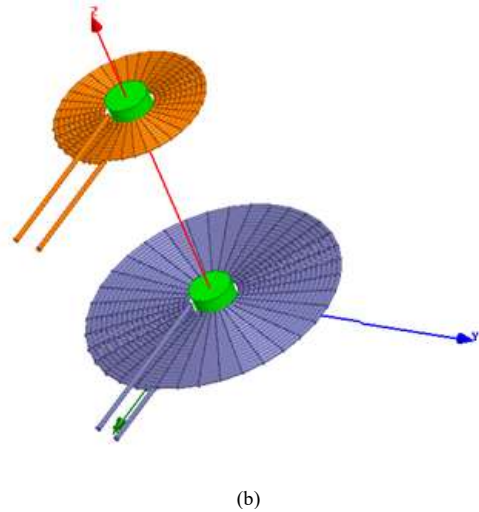
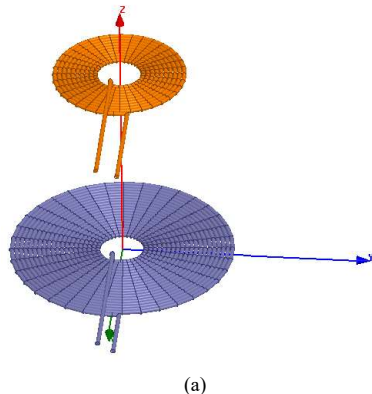


Fig. 5. Circular planar coil (a) without ferromagnetic core (b with ferromagnetic core)

Increment in inductances gives a high value of the coupling coefficient,  $k$ . As per the analysis the coupling coefficient has been increased approximately by 3.233 times for rectangular coil with air core whereas for ferromagnetic core this has been increased approximately 6.75 times. For better

**Table 2: Coil Parameters**

Parameters	Circular		Rectangular	
Core type	Air	M43_29G	Air	M43_29G
Coupling coefficient, $k$	2.42E-05	6.59E-05	7.8 E-05	44.54E-05
Mutual inductance, $M$	1.51nH	8.19 nH	11.97 nH	155.864 nH
Self-Inductance TC	12.574 $\mu$ H	467.255 $\mu$ H	26.4244 $\mu$ H	1.27056mH
Self-Inductance RC	30.8326 nH	26.4244 $\mu$ H	895.466nH	96.3393 $\mu$ H
Flux on RC (mWb)	0.043	0.046	0.636	1.93

understanding, a comparative study between circular and rectangular coils with ferromagnetic material is shown in the Fig. 9. Study of mutual inductance, coupling coefficient, self-inductances of TC and RC and induced flux in the RC has been illustrated in Fig.9 (a), (b), (c), (d), (e) respectively.

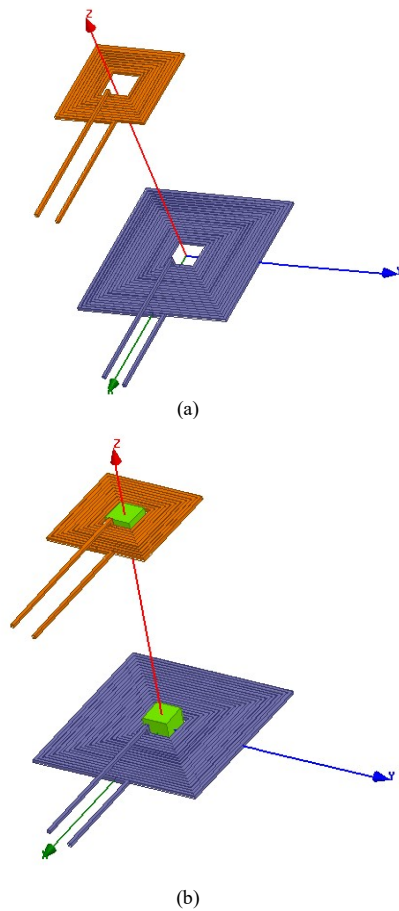


Fig. 6. Rectangular planar coil (a) without ferromagnetic core (b) with ferromagnetic core

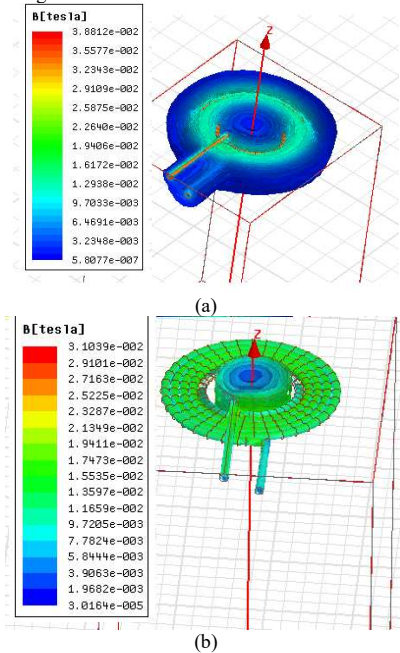


Fig. 7. Flux density distribution of circular planar coil (a) without ferromagnetic core (b) with ferromagnetic core

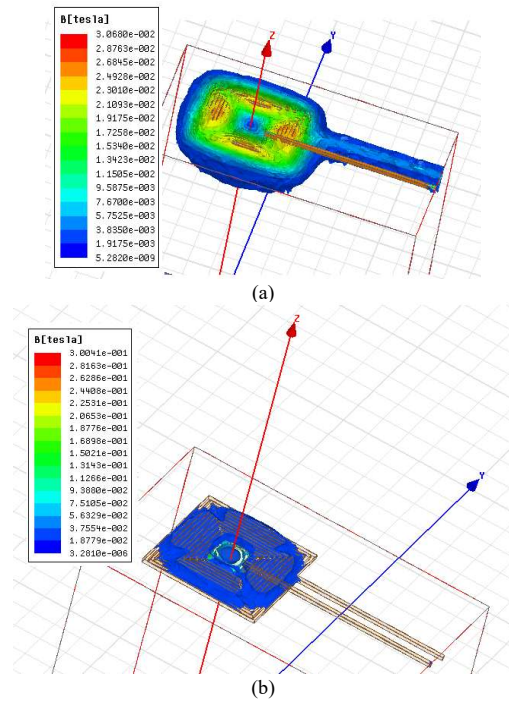
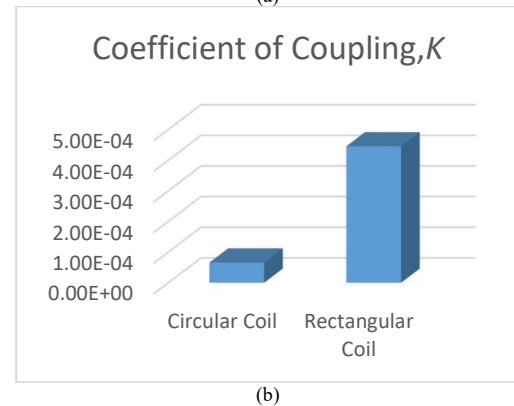
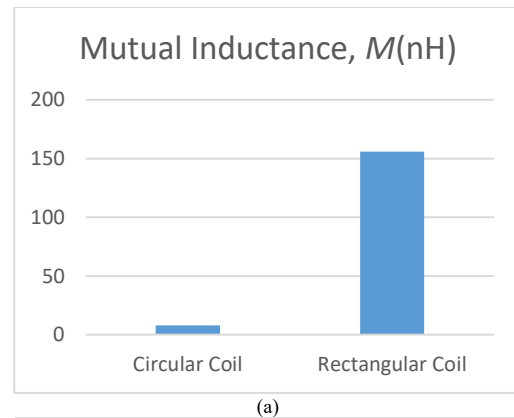
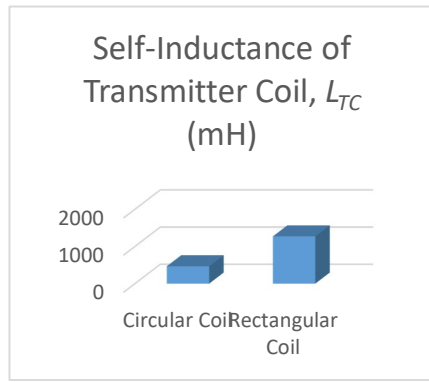
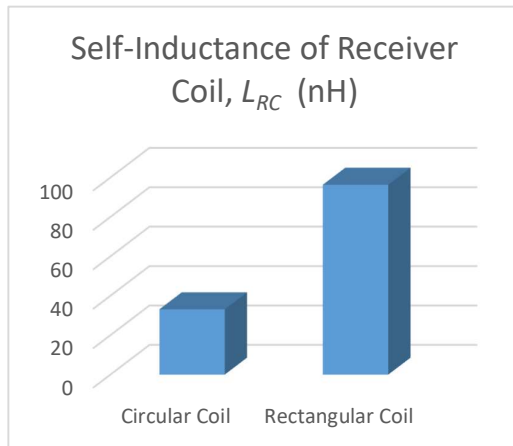


Fig. 8. Flux density distribution of rectangular planar coil (a) without ferromagnetic core (b) with ferromagnetic core

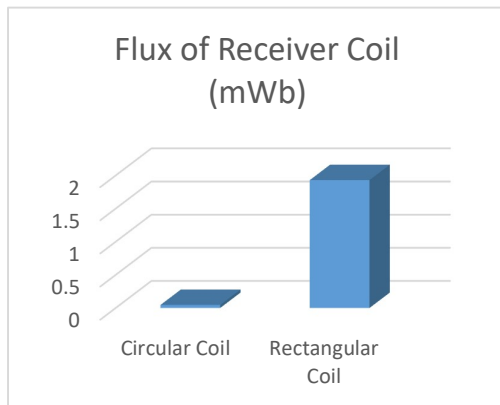




(c)



(d)



(e)

Fig. 9. Comparative analysis of different parameters for Circular and Rectangular coils with M43\_29G.

#### IV. CONCLUSION

The prime components of an inductive wireless power transfer system for charging batteries of electric vehicles are the transmitter and receiver coils. The mutual inductances and the coils' coupling coefficients significantly affect the wireless power transfer. The magnitudes of the inductances are dependent on the shape of the coils. The circular and the rectangular shape of the transmitter and receiver coils have been analysed here in Ansys Maxwell 3-D environment. The finite element analysis (FEA) was conducted in Magnetostatics mode. The results revealed the mutual

inductances for the rectangular coil is higher than that of the circular coil. Again, the inductances of the receiver and transmitter coil increased when ferromagnetic cores were used, and hence, the system flux improved. The Maxwell analysis showed the flux density distribution of the receiver coil. This gives the value of the flux density on the receiver coil as the maximum for a rectangular coil set with a ferromagnetic core. In this work, the misalignment of the coils has not been considered. This could be included as a future work.

#### REFERENCES

- [1] V. Ramakrishnan *et al.*, "Design and implementation of a high misalignment-tolerance wireless charger for an electric vehicle with control of the constant current/voltage charging," *Sci. Rep.*, vol. 14, no. 1, pp. 1–28, 2024, doi: 10.1038/s41598-024-63952-6.
- [2] J. K. Nama, A. K. Verma, M. Srivastava, and P. S. Tomar, "An Efficient Inductive Power Transfer Topology for Electric Vehicle Battery Charging," *IEEE Trans. Ind. Appl.*, vol. 56, no. 6, pp. 6925–6936, 2020, doi: 10.1109/TIA.2020.3018419.
- [3] V. Sari, "Design and Implementation of a Wireless Power Transfer System for Electric Vehicles," *World Electr. Veh. J.*, vol. 15, no. 3, 2024, doi: 10.3390/wevj15030110.
- [4] A. A. S. Mohamed, A. Berzoy, F. G. N. De Almeida, and O. Mohammed, "Modeling and Assessment Analysis of Various Compensation Topologies in Bidirectional IWPT System for EV Applications," *IEEE Trans. Ind. Appl.*, vol. 53, no. 5, pp. 4973–4984, 2017, doi: 10.1109/TIA.2017.2700281.
- [5] K. E. I. Elnail, X. Huang, C. Xiao, L. Tan, and X. Haozhe, "Core structure and electromagnetic field evaluation in wpt systems for charging electric vehicles," *Energies*, vol. 11, no. 7, pp. 1–17, 2018, doi: 10.3390/en11071734.
- [6] R. Bosshard, J. Muhlethaler, J. W. Kolar, and I. Stevanovic, "Optimized magnetic design for inductive power transfer coils," *Conf. Proc. - IEEE Appl. Power Electron. Conf. Expo. - APEC*, pp. 1812–1819, 2013, doi: 10.1109/APEC.2013.6520541.
- [7] C. W. Yang and C. L. Yang, "Analysis of inductive coupling coils for extending distances of efficient wireless power transmission," *2013 IEEE MTT-S Int. Microw. Work. Ser. RF Wirel. Technol. Biomed. Healthc. Appl. IMWS-BIO 2013 - Proc.*, pp. 2–4, 2013, doi: 10.1109/IMWS-BIO.2013.6756177.
- [8] R. Basak, "Optimizing single-phase transformer design parameters using stochastic methods : a performance evaluation study with a broad-based review and analysis," *International Journal of Communication, Science and Technology*, vol. 1, no. 1, pp. 1–18, 2024.
- [9] A. Eikani, M. Amirkhani, E. Farmahini Farahani, V. Pickert, M. Mirsalim, and S. Vaez-Zadeh, "Robust Wireless Power Transfer for EVs by Self-Oscillating Controlled Inverters and Identical Single-Coil Transmitting and Receiving Pads," *Energies*, vol. 18, no. 1, pp. 1–21, 2025, doi: 10.3390/en18010211.
- [10] E. S. Gámez Rodríguez, A. K. RamRakhyani, D. Schurig, and G. Lazzi, "Compact Low-Frequency Metamaterial Design for Wireless Power Transfer Efficiency Enhancement," *IEEE Trans. Microw. Theory Tech.*, vol. 64, no. 5, pp. 1644–1654, 2016, doi: 10.1109/TMTT.2016.2549526.
- [11] H. Yoda, "Development of WPT Systems for Railway Vehicles and Study for Low-Frequency Application," *Proc. 2024 IEEE Wirel. Power Technol. Conf. Expo, WPTCE 2024*, pp. 536–541, 2024, doi: 10.1109/WPTCE59894.2024.10557361.
- [12] M. Tampubolon, H. J. Chiu, H. C. Hsieh, J. Y. Lin, and Y. C. Hsieh, "High-efficiency bidirectional resonant WPT system for electric vehicles," *Int. J. Power Electron. Drive Syst.*, vol. 14, no. 2, pp. 948–959, 2023, doi: 10.11591/ijpeds.v14.i2.pp948-959.
- [13] N. Prosen and J. Domajnko, "Optimization of a Circular Planar Spiral Wireless Power Transfer Coil Using a Genetic Algorithm," *Electron.*, vol. 13, no. 5, 2024, doi: 10.3390/electronics13050978.